Influence of NaOH, Ni/Al$_2$O$_3$ and Ni/SiO$_2$ catalysts on hydrogen production from the subcritical water gasification of model food waste compounds

Rattana Muangrat, Jude A. Onwudili, Paul T. Williams *

Energy and Resources Research Institute, The University of Leeds, Leeds LS2 9JT, United Kingdom

ARTICLE INFO

ABSTRACT

The production of hydrogen via subcritical water gasification of model food waste compounds, glucose and glutamic acid representing carbohydrate and protein has been studied. The influence of NaOH additive, Ni/Al$_2$O$_3$ and Ni/SiO$_2$ catalysts and combinations of these catalysts in relation to hydrogen production was investigated at a temperature of 330 °C and 13.5 MPa pressure. Generally, glucose produced more hydrogen gas than glutamic acid even with NaOH. Hydrogen production from the model food waste compounds in the presence of NaOH was superior to that of the investigated nickel catalysts supported on SiO$_2$ and Al$_2$O$_3$. The production of hydrogen gas increased when NaOH was added, whereas other gases, CO, CO$_2$ and hydrocarbons (C$_1$–C$_4$) decreased with increasing concentration of NaOH. Combination of the catalysts Ni/SiO$_2$ or Ni/Al$_2$O$_3$ with NaOH alkali only slightly increased hydrogen production. The addition of NaOH reduced the amount of CO$_2$, and tar produced during subcritical water gasification of the model compounds, unlike when Ni/SiO$_2$ and Ni/Al$_2$O$_3$ catalysts were used. Furthermore NaOH decreased the amount of carbon deposited on the Ni/SiO$_2$ and Ni/Al$_2$O$_3$ catalyst surface. However the formation of dawsonite was confirmed and provided experimental evidence of the reaction of sodium hydroxide with alumina in Ni/Al$_2$O$_3$, with a potential for decreased catalytic activity.

© 2010 Elsevier B.V. All rights reserved.

1. Introduction

Generation of hydrogen from biomass and biomass-derived waste is a benign method to produce clean energy [1]. Biomass wastes include food waste, wood, and agricultural residues and have a highly varied composition depending on source. The varieties of components inside biomass waste involve a complexity of reaction mechanisms which may occur between different components when they are used during the various gasification processes [2]. As a result, many researchers do not often investigate real-world biomass samples but rather study the conversion of model compounds derived from biomass such as glucose, cellulose or fructose [3].

Biomass such as food waste contains not only carbohydrate but also substantial amounts of protein [4]. For example, glycine has been studied as a model compound for proteins [5,6]. Douda and Basiuk [7] studied the pyrolysis of amino acids in relation to the recovery of the starting materials and yields of condensation products. They found that amino acids decompose to mainly simple inorganic compounds such as CO$_2$, H$_2$O, NH$_3$ and CO and a variety of volatile organic compounds [7]. Xu et al. [8] showed that it

was feasible to produce hydrogen from biomass or organic matter containing protein or lipids.

Subcritical and supercritical water gasification has become an attractive method to generate hydrogen from biomass [9]. Water, heated above its boiling point to between 200 and 374 °C, and held under sufficient pressure to maintain its liquid state is known as subcritical water [10,11]. However, many researchers have referred to subcritical water at temperatures from 300 °C to just below the critical point of water (T_c = 374 °C and P_c = 22.1 MPa), as near-critical water [12,13]. This paper focuses on the partial oxidative gasification at temperature and pressure of two model compounds 330 °C and 13.5 MPa, respectively, in the presence of catalysts. Hence, the reaction medium may be described interchangeably as subcritical or near-critical water.

The advantages of near-critical water as a solvent and reactant include decreases in dielectric constant, thermal conductivity, ion products, viscosity, and density. In addition, organic compounds become highly soluble and gases are also miscible in the supercritical water region. High water content in the raw material under supercritical conditions would promote gasification reactions and production of fuel gas [14–16]. The reaction rates are intrinsically fast in subcritical and supercritical water conditions [17].

The subcritical and supercritical water gasification of wet biomass such as food waste is more advantageous than conventional gasification because it does not require a drying step.

Conversion of this wet waste material via hydrothermal gasification would enhance the economics of the operation. The process generates hydrogen and small quantities of carbon monoxide [18]. Kruse [4] found that the energy required to attain hydrothermal gasification conditions of 600 °C and 30 MPa was only slightly lower than the energy required to dry wet biomass for conventional 'dry' gasification at 600 °C and 0.1 MPa. However, the same author showed that at much lower temperatures between 200 and 450 °C, the energy required for hydrothermal gasification of wet feedstocks becomes significantly lower compared to evaporation and dry gasification. This is an obvious advantage plus the fact that the energy used in hydrothermal process is held at high pressure which makes it largely recoverable. It is therefore important to aim for a hydrothermal gasification process of wet feedstocks at temperatures below or around 450 °C.

Subcritical water gasification operating at lower temperature requires the use of alkali salts or catalysts to enhance hydrogen production and prevent the formation of polymeric materials and finally char [19]. Rossum et al. [20] found that a catalyst was required in hydrothermal gasification at low temperature. Catalysts use can increase the desired chemical reaction rate and control the product distribution. Many studies have investigated hydrogen production from biomass or model compounds with catalysts such as KOH, NaOH, K_2CO_3, Na_2CO_3, Ni catalysts and activated carbon [21]. Nickel is the most widely used catalyst in industry [22] due to its lower cost [23]. Many researchers have used Ni-based catalysts in biomass gasification because they are effective for tar reduction, char prevention and hydrogen production [24–27]. Nickel catalysts have been found to enhance the water–gas shift reaction [28], methanation [29–33] and hydrogenation reactions [34]. In addition, Ni catalysts have been used in the sub- and supercritical water gasification of biomass [35–37], and have been found to tend to promote methane production. Yoshida et al. [35] conducted supercritical water gasification of lignin, cellulose and their mixture in the presence of a Ni catalyst at 400 °C and obtained methane and carbon dioxide as the major gaseous products. Minowa and Ogi [38] studied the effect of a reduced Ni catalyst on the gasification of cellulose in subcritical water and reported that the yield of CH_4 was enhanced, whereas the yield of H_2 was suppressed by the methanation reaction in the presence of Ni. On the other hand, there are many researches using homogeneous catalysts such as NaOH and KOH because they dissolve in subcritical water and have been shown to effectively gasify biomass to produce hydrogen gas [39]. For example, Watanabe et al. [1] reported that NaOH catalysed and promoted hydrogen generation during the supercritical water gasification of cellulose, glucose and lignin.

In this paper, glucose, glutamic acid and a mixture of glucose and glutamic acid being representative model compounds of carbohydrate and protein have been gasified under subcritical water gasification conditions for hydrogen gas production. While several reports [19,35–39,1] have highlighted the separate effects of nickel-based catalysts and alkali catalysts on hydrothermal gasification, there is hardly any reports in literature on the catalytic effects of combined nickel-based and alkali catalysts. NaOH has the potential to reduce or suppress char and tar formation along with high H_2 gas yield during low temperature hydrothermal gasification. It is therefore important to investigate the catalytic activity of homogenous NaOH catalyst/additive in the presence of heterogeneous silica- and alumina-supported Ni catalysts. This investigation is thus focused on the catalytic performance of Ni/Al_2O_3, Ni/SiO_2 and NaOH in the production of hydrogen and/or methane gases. The Ni catalysts were used individually or in combination with NaOH, and the results compared with NaOH alone. This possibility of chemical interaction between the nickel-based catalysts and NaOH, and the implication of such interactions on the gasification process has also been outlined.

2. Material and methods

2.1. Raw materials and reactants

The food waste model compounds used were anhydrous D-(+)-glucose (99%) obtained from Alfa Aesar, UK and L-glutamic acid obtained from Sigma–Aldrich, UK. Elemental analysis of the model compounds showed that glucose consisted of 40.4% carbon, 7.20% hydrogen and 52.2% oxygen, while glutamic acid was composed of 40.7% carbon, 6.15% hydrogen, 8.95% nitrogen and 43.8% oxygen. The oxidant used as a source of oxygen (hydrogen peroxide, 30% w/v) was obtained from Sigma–Aldrich, UK. Sodium hydroxide pellets (purity 99%) from Sigma–Aldrich, Ni/Al_2O_3 and Ni/SiO_2 were used as catalyst. The Ni-based catalysts were prepared by the impregnation method.

2.2. Preparation of catalysts

SiO_2 (Sigma–Aldrich, UK) and Al_2O_3 (Fisons Scientific Equipment, UK) were impregnated with an aqueous solution of $Ni(NO_3)_2 \cdot 6H_2O$ (Sigma–Aldrich, UK) and the resulting solution was mixed and stirred at a controlled temperature of 70 °C until the solution became thickened via water evaporation. The catalyst was dried at 110 °C overnight. Each impregnated and dried catalyst (consisting of 6.23 wt% Ni) was then calcined at a temperature of 400 °C in air for 3 h. The catalyst was cooled to room temperature and then crushed and sieved to a size of less than 0.211 mm.

2.3. Characterization of catalysts

The BET (Brunauer, Emmett, and Teller) surface area of each catalyst was obtained via nitrogen adsorption experiments using a Micromeritics Tristar 3000 automated gas adsorption analyser (Micromeritics Instrument Co.). The BET surface area of the Ni/SiO_2 and Ni/Al_2O_3 catalysts was 5.98, and 94.8 $m^2 g^{-1}$, respectively.

Thermogravimetric experiments are carried out with a TGA 50, Shimadzu Scientific instrument to investigate the thermal degradation characteristics of the model compounds and the used catalysts. The sample, around 10–15 mg, was heated in nitrogen at 10 °C min⁻¹ from room temperature to 110 °C with a hold time of 10 min, followed by heating to 920 °C and held at that temperature for a period time of 40 min before switching to air with a hold time of 20 min.

X-ray diffraction (XRD) was used to characterize the catalysts and the instrument used was a Phillips PW1050 Goniometer with a Philips PW1730generator with a CuKa radiation X-ray tube. The sample was finely ground to less than 75 mm size and loaded into the 20 mm aperture of an aluminium sample holder. The instrument was equipped with a Hiltonbrooks' HBX data acquisition software system to collect the data. GBC Scientific Equipment Ltd's TRACES software using ICDD PDF2 (International Centre for Diffraction Data Powder Diffraction Files) database was used for phase identification.

Scanning electron microscopy (SEM) was also used to characterize and examine the catalysts. A higher resolution SEM (LEO 1530) coupled to an energy dispersive X-ray spectrometry (EDXS) system was used to determine the characteristic elements in the solid residues.

2.4. Reactor system and experimental procedure

The subcritical water gasification of the model compound samples was investigated in a stainless steel reactor obtained from the Parr Instrument Co., Moline, IL, USA. The schematic of the reactor has been reported earlier [16]. Briefly, the reactor has 500 ml of volume capacity and a maximum operating temperature and pressure

of the reactor was 500 °C and 26 MPa, respectively. A cylindrical tube attached at the end of gas outlet was used for sampling gas products.

In each case, a total of 5 g of sample and catalysts were weighed into the reactor and mixed with a known 95 ml of deionized water and 5 ml of hydrogen peroxide bringing the total volume of liquid to 100 ml. The amount of each catalyst used was 4 g each. In the case of NaOH, dissolving 4 g in 100 ml aqueous solution represented a 1 M solution of the alkali. The residual air in the reactor was purged with argon for 10 min. After purging, the reactor was heated to the set temperature of 330 °C at a heating rate of 20 °C per minute. The pressure of the reactor could not be adjusted manually because the reactor was a closed system and therefore the reaction pressure depended on the reaction temperature and water loading in the reactor. The initial volume of liquid charged into the reactor provided an autogenic pressure of 13.5 MPa at the reaction temperature of 330 °C. The reaction can be successfully held at these conditions for extended reaction times without any significant variation. At the end of each experiment, the heating was stopped and the reactor was removed from the heater and cooled to room temperature by an air cooling system. After cooling, the ambient temperature and pressure exerted by the produced gas were recorded by reading from the thermocouple and pressure gauge, respectively. The ambient temperature and final pressure on cooling were used to calculate mass of each gas products. The gas outlet valve was opened to collect the gas samples using gas-tight plastic syringes that can be fitted with gas-tight stopper. After the gas sampling, the reactor was opened to sample the liquid sample and solid residues (where present). The volume of liquid effluent recovered was measured and noted.

2.5. Product analysis

2.5.1. Gas analysis

The effluent gas sampled into a gas-tight syringe was immediately analysed using two separate gas chromatographs. A Varian CP-3380 gas chromatograph with a thermal conductivity detector (GC/TCD) and fitted with two columns was used. One column was used to separate hydrogen, oxygen, nitrogen, and carbon monoxide while the other column was used for analyzing carbon dioxide. The columns used were 2 m long with 2 mm diameter, packed a 60–80 mesh molecular sieve. Argon was used as the carrier gas. Hydrocarbon gases from C_1–C_4 were analysed using a second Varian CP-3380 gas chromatograph with flame ionization detector (GC/FID). The column used was a 2 m long by 2 mm diameter and packed with 80–100 mesh Hayesep packing material. Nitrogen was used as the carrier gas. In each case, 1 ml of the sampled gas was injected directly, using a 1 ml SGE syringe, into the gas chromatographs from the gas-tight plastic syringes. The results from the GCs were obtained in volume %. The measured volume of liquid effluent (between 95 and 97 ml) was used to calculate the volume occupied by the produced gas. The amount of gases dissolved in the liquid effluent was estimated using Henry's Law. We used the final temperature (room temperature) and pressure (ca 0–10 bar) of the reactor after cooling to calculate the mass of each gas produced based on the general gas equation.

2.5.2. Liquid and solid analysis

Liquid sample and solid residue consisting of tar, char and spent catalysts (Ni/Al$_2$O$_3$ or Ni/SiO$_2$), and an aqueous phase containing water soluble products (TWSP) were produced from the reaction. The char or char mixed with catalyst was separated by filtration. The tar was extracted from the water using a separating funnel and extracted with ethyl acetate by shaking vigorously for 5 min. The combined organic phase and aqueous phase were allowed to stand in the separating funnel and followed by separation of the
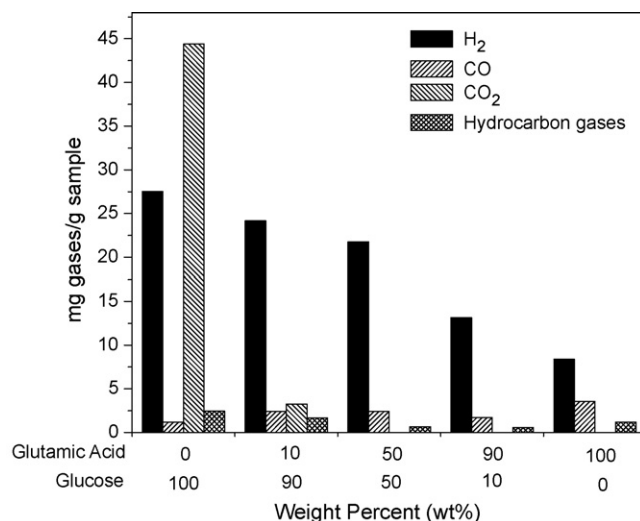

Fig. 1. Gas production from different weight ratio of glucose and glutamic acid in the presence of 4 g NaOH at 330 °C, 120 min of reaction time and 1.5 wt% H$_2$O$_2$.

immiscible phases. The ethyl acetate extract layer (organic phase) containing oil/tar components was blown to dryness with a gentle nitrogen gas stream, placed in a desiccator to dry overnight, and then weighed to determine the total mass of oil/tar produced. The mass of total water soluble products was determined by taking an aliquot of aqueous phase and then placed in a crucible on a water bath to evaporate the water. After evaporating the water, the crucible was dried in an oven at 105 °C overnight to determine the mass of total water soluble products (TWSP). The amount of water produced from the decomposition of hydrogen peroxide to water and oxygen was calculated. The mass balance was based on the total mass of the reactants (feed).

3. Results and discussion

3.1. Influence of different weight ratios on the subcritical water gasification of glucose and glutamic acid
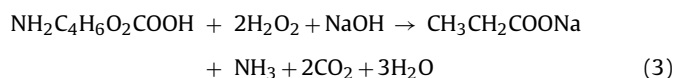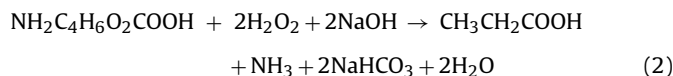
Fig. 1 shows the gas composition and yield for the subcritical water gasification of glucose, glutamic acid and various mixtures of these model compounds in the presence of NaOH and H$_2$O$_2$ at 330 °C and 120 min residence time. The total quantity of feed material used in each experiment was 5 g and this was reacted in 100 ml of liquid (95 ml of deionized water and 5 ml of hydrogen peroxide). The ratio of the two model compounds was expressed in terms of the percentage of each compound in the total feed used in each experiment. For example, where only glucose or glutamic acid was used, the percentage ratio is expressed as 100. A 50:50 ratio represents equal quantities of the compounds at 2.5 g each.

The probable predominant reaction equations for subcritical water gasification of glucose and glutamic acid in the presence of NaOH and H$_2$O$_2$ are proposed as follows:

Partial oxidation of glucose in the presence of NaOH:

$$C_6H_{12}O_6 + 6H_2O_2 + 6NaOH \rightarrow 6HCOONa + 12H_2O \tag{1}$$

Partial oxidation of glutamic acid could occur in two ways;

$$NH_2C_4H_6O_2COOH + 2H_2O_2 + 2NaOH \rightarrow CH_3CH_2COOH$$
$$+ NH_3 + 2NaHCO_3 + 2H_2O \tag{2}$$

$$NH_2C_4H_6O_2COOH + 2H_2O_2 + NaOH \rightarrow CH_3CH_2COONa$$
$$+ NH_3 + 2CO_2 + 3H_2O \tag{3}$$

$$CH_3CH_2COOH + H_2O \rightarrow lowercarboxylicacids$$
$$+ \ hydrocarbongases \qquad (4)$$

$$CH_3CH_2COONa + H_2O \rightarrow lowercarboxylicacidsalts$$
$$+ \ hydrocarbongases \qquad (5)$$
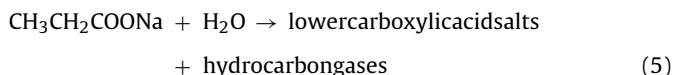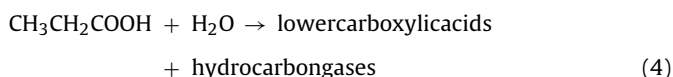
(*Note*: Eqs. (4) and (5) are not stoichiometric)

Subsequent reactions:
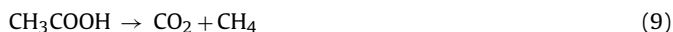
Decarbonylation reaction of the carboxylic acid salts:

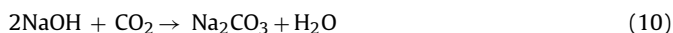$$HCOONa \rightarrow CO + NaOH \qquad (6)$$

Water–gas shift reaction:

$$CO + H_2O \rightarrow CO_2 + H_2 \qquad (7)$$

Dehydration reaction of the carboxylic acids:

$$HCOOH \rightarrow CO + H_2O \qquad (8)$$

Decarboxylation of the carboxylic acids

$$CH_3COOH \rightarrow CO_2 + CH_4 \qquad (9)$$

CO_2-capture reaction:

$$2NaOH + CO_2 \rightarrow Na_2CO_3 + H_2O \qquad (10)$$

In hydrothermal degradation, proteins are very rapidly hydrolyzed to amino acids. Degradation of amino acids takes place by decarboxylation to produce carbonic acid and amines or by deamination to produce ammonia and organic acid [21]. The degradation of an organic acid produces mainly CO, CO_2, H_2 and water. The use of a catalyst potentially has a significant effect on both the ratio of deamination and/or decarboxylation and on the extent of degradation of organic acid [40]. Results obtained in this work suggest that subcritical water gasification of glutamic acid produced CO_2 from two possible ways: decarboxylation of the carboxylic acid groups, and the water gas shift reaction involving CO. When reacted, glutamic acid could decompose mainly to CO_2 from decarboxylation of the carboxylic acid functional groups. In the presence of NaOH, it would appear that much of the alkali was consumed by its neutralization reaction with the carboxylic acid groups in glutamic acid. Even if the decarboxylation of glutamic acid were to occur first before any reactions with NaOH, much of the alkali would be consumed in the formation of Na_2CO_3 or $NaHCO_3$. Interestingly, no CO_2 was detected when glutamic acid was 100% of the feed (i.e. using 5 g glutamic acid). For complete neutralization, 5 g of glutamic acid would require about 2.72 g of NaOH, hence the amount of alkali used (4 g) was more than sufficient to neutralize the acid. Therefore, the yield of H_2 gas from glutamic was still higher in the presence of NaOH than without the alkali, indicating that some residual NaOH was able to decompose the –C–C–chain to produce gasifiable intermediates. Meanwhile, when 5 g (as 100% of feed) of glucose was gasified under same experimental condition produced higher, much more H_2 and CO_2 yields were obtained in the gaseous product. This may indicate that much of the NaOH applied was available to decompose the glucose to intermediates such as sodium formate, which could produce hydrogen gas [12,19]. In addition, any water–gas shift reaction would be accelerated in the forward direction by NaOH capturing CO_2 to produce higher H_2 gas yield. In this case, about 44.4 mgCO_2/g of glucose was still obtained, indicating that the amount of alkali used was not sufficient to capture all the CO_2 produced. Onwudili and Williams [19] have suggested that the ratio of alkali (NaOH) to biomass feed (glucose) shouldbe in the region of 1.2, for com-

plete degradation biomass to gasifiable intermediates with no CO_2 produced.

In this work, it can be concluded that glucose could react with NaOH to degrade to intermediates which gave higher yields of CO via partial oxidation reactions. The CO would be forward catalysed via the water–gas shift reaction by NaOH to produce higher H_2 yield through the water–gas shift reaction. Much more hydrogen gas was produced from glucose compared to glutamic acid in this work. Consequently, it was not surprising that the yield of hydrogen began to fall when the feed was a mixture of glutamic acid and glucose.

Fig. 1 shows that when the amount of glutamic acid was higher compared to glucose, the hydrogen and hydrocarbon gas yield decreased, whereas the amount of CO slightly increased or hardly changed. This suggests that the main CO product was produced via the dehydration reaction of formic acid shown in Eq. (8) when the weight percentage of glutamic acid was higher. However, the yield of CO_2 gas product was below the detection level when the mixture of glucose and glutamic acid contained a lower ratio of glucose or higher ratio of glutamic acid.

While the added NaOH was available to remove carbon dioxide during the reaction involving only glucose, in reactions involving glutamic acid, two possible reactions could occur. Firstly, the glutamic acid could react directly with sodium hydroxide to form a sodium salt of glutamic acid (sodium glutamate) via neutralization/condensation reaction as shown in Eq. (3). Secondly, the glutamic acid could undergo decarboxylation to produce carbon dioxide which then reacted with the added NaOH. In either of these ways, the added NaOH appear to be consumed in reactions other than the decomposition of the glutamic acid to lower carboxylic acid salts which are important for hydrogen and methane production [19]. The absence of these intermediate compounds, particularly sodium formate, may be linked to the low hydrogen gas production from feed samples containing glutamic acid.

As demonstrated in Fig. 1, when the ratio of glucose/glutamic acid was 1:1, the yield of H_2 gas product was still low, possibly because of the consumption of added alkali by side reactions, e.g. neutralization reaction with glutamic acid. On the other hand chemical reaction between an amino acid and a reducing sugar such as glucose may occur during hydrothermal gasification. Amines as degradation products of proteins and consecutive products of carbohydrate splitting react with each other to form N-heterocyclic compounds which easily form rather stable free radical cations acting as free radical scavengers in the reaction mixture leading to unexpectedly low gas formation [4]. Therefore, H_2 production relied heavily more from the reaction of glucose than glutamic acid. However, the presence of glutamic acid could suppress the reaction of glucose with sodium hydroxide as well. Kruse et al. [18] have reported that the presence of proteins tended to have a negative impact on hydrogen production from carbohydrate biomass. The gas products in the presence of glutamic acid were much lower compared to experiments without this compound. Amino acids decompose to form small traces of CO [21]. This CO could be consumed through the water–gas shift reaction under the right conditions. This suggests that a small amount of CO produced would lead to the production of a small amount of H_2 and CO_2 generation as well. However, the catalysis of the water–gas shift reaction by NaOH also depended on the capture of carbon dioxide as sodium carbonates/bicarbonate. This indicates that in the presence of sodium ions, the amount of CO_2 in the gas phase would reduce to even zero depended on the amount of sodium ions available [19]. Hence, the conversion of CO would accurately be measured by H_2 yield rather than CO_2 yield, under alkaline hydrothermal gasification.

Table 1
Gas Production from 5.0 g loading of model compounds without and with catalysts at 330 °C, 120 min of reaction time and 1.5 wt% H_2O_2 each.

Sample types and experimental conditions	Gas production (mg gases/g of sample)			
	H_2	CO	CO_2	Hydrocarbon gases (C_1–C_4)
5 g glucose				
Without catalyst	3.17	27.4	419.3	5.18
NaOH	27.5	1.18	44.41	2.43
Ni/Al_2O_3	5.63	30.0	558.4	7.75
Ni/SiO_2	4.36	29.0	456.9	8.26
NaOH + Ni/Al_2O_3	26.1	8.86	–	7.68
NaOH + Ni/SiO_2	23.2	2.27	51.9	2.04
5 g glutamic acid				
Without catalyst	3.00	13.01	520.8	–
NaOH	8.37	3.55	–	1.21
Ni/Al_2O_3	1.98	13.8	536.6	7.41
Ni/SiO_2	1.75	15.7	603.3	8.75
NaOH + Ni/Al_2O_3	6.85	2.92	0.36	0.60
NaOH + Ni/SiO_2	6.01	3.11	30.4	0.61
2.5 g glucose + 2.5 g glutamic acid				
Without catalyst	2.00	5.91	558.6	3.78
NaOH	24.2	2.21	–	0.83
Ni/Al_2O_3	2.89	21.8	639.1	7.15
Ni/SiO_2	3.26	19.2	639.3	8.11
NaOH + Ni/Al_2O_3	17.9	0.74	63.0	1.21
NaOH + Ni/SiO_2	15.7	1.45	–	1.16

3.2. Influence of NaOH, Ni/Al_2O_3 and Ni/SiO_2 on gas composition from subcritical water gasification of glucose and glutamic acid

The influence of NaOH and the two nickel catalysts, Ni/Al_2O_3 or Ni/SiO_2 on the yield of hydrogen and other gases on the subcritical water gasification of glucose alone, glutamic acid alone and a 1:1 mixture of glucose and glutamic acid were investigated. The reaction temperature was 330 °C, pressure of 13.5 MPa, and 120 min reaction time. The amount of nickel in the catalysts was constant at 6.23 wt% of Ni. Table 1 shows the results of the gas products obtained. The additive, NaOH, resulted in a higher production of hydrogen gas compared with only Ni/SiO_2 or Ni/Al_2O_3 catalyst. Moreover, the addition of only NaOH produced hydrogen at a higher yield than the combination of the catalysts (NaOH and Ni/SiO_2 or NaOH and Ni/Al_2O_3).

The Ni/SiO_2 or Ni/Al_2O_3 catalysts used in this study, their NiO component could be reduced to Ni by deposited carbon ($NiO + C \rightarrow Ni + CO$). It is thus possible that Ni particles might not have good contact with water-soluble products considered as intermediates to produce hydrogen (water-soluble products $\xrightarrow{Ni}$ H_2 + CO_2) [34]. Fang et al. [41] studied hydrogen production from cellulose and glucose in both batch and flow reactors under hydrothermal gasification at 400 °C with and without catalysts (Ni, Ru and Pt), they found that in the case of using a 50 nL optical micro-reactor, the rate of hydrothermal gasification of glucose and cellulose with Ni catalysts was low, and produced a high amount of solid residue and oil due to a limitation of phase contact between the heterogeneous catalyst Ni phase and dissolved solutes. Moreover, Rossum et al. [20], experienced difficulty in converting biomass using catalytic gasification in a single vessel reactor. They suggested that the catalysts suffered from inefficient contact between the catalyst and biomass (due to the texture of the biomass). Therefore, it is possible that the catalysts, Ni/SiO_2 and Ni/Al_2O_3, being heterogeneous catalyst, may not effectively contact with the gas phase where water–carbon reaction and the water–gas shift reaction occur. As a result, the combination of the two catalysts (NaOH and Ni/Al_2O_3 or NaOH and Ni/SiO_2) generated a lower hydrogen yield than when the NaOH catalyst was used alone. Ishida et al. [9] studied the effect of the additives, Na_2CO_3 and Ni/SiO_2 on the hydrothermal gasification of cellulose at a temperature of 400 °C. Although the combination of these two catalysts led

to higher selective hydrogen production by dissolving CO_2 into the liquid layer, a large amount of additives were required to generate a hydrogen yield with significantly higher selectivity.

According to the water–gas shift reaction, increases in both the CO_2 and H_2 concentrations are expected by the addition of a suitable catalyst. The addition of either mixed catalysts, NaOH and Ni/Al_2O_3 or NaOH and Ni/SiO_2 led to an increase in the amount of H_2 product compared to that obtained using only Ni/Al_2O_3 or Ni/SiO_2. In the case of additive NaOH, the decrease in CO_2 production is most likely due to its capture by NaOH and associated with the dissolution of CO_2 in the aqueous medium forming sodium carbonate salts, sodium bicarbonate and/or free carbonate ions in the liquid phase. This result indicates that the NaOH is effective in the generation of H_2 via the promotion of water–gas shift reaction [19]. Lower concentration of CO was detected in experiments with NaOH compared to experiments without the alkali because the alkali promoted the consumption of CO via the water–gas shift reaction.

Fig. 2 shows the percent recovery of H_2 product, represented as the theoretical potential of H_2 that could be obtained from
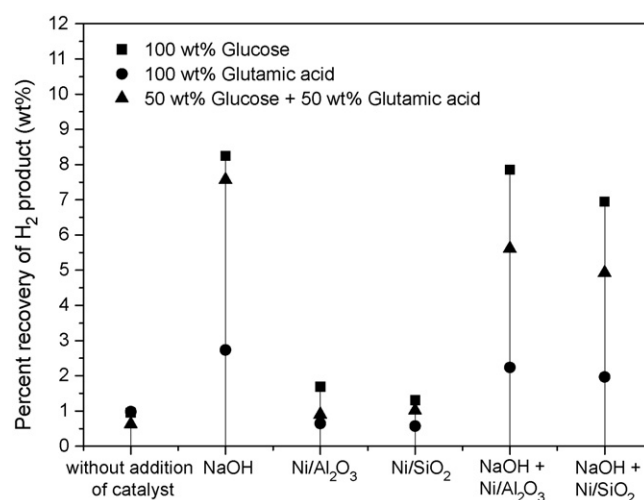

Fig. 2. Percent recovery of H_2 product from subcritical water gasification of glucose only, glutamic acid only and 1:1 glucose/glutamic acid mixture without and with catalysts at 330 °C, 120 min and 1.5 wt% H_2O_2.

the sample. In this paper, the theoretical potential H_2 production corresponded to the maximum H_2 gas production for the 100% conversion of the hydrogen contained in the glucose, glucose/glutamic acid mixture and glutamic acid. These maximum hydrogen yields would be 333 mg/5 g for glucose alone, 306.1 mg/5 g for glutamic acid alone and 319.7 mg for the mixture of 2.5 g glucose and 2.5 g glutamic acid. Based on the H_2 yields, subcritical water gasification of the model compounds the order of their potential H_2 gas production was glucose > the mixture of glucose and glutamic acid > glutamic acid.

The total mass balances for products obtained during the subcritical water gasification of glucose, glutamic acid and glucose mixed with glutamic acid are presented in Tables 2–4, respectively. At each condition, the addition of NaOH resulted in the significant decrease in the yields of tar and char, much in the same manner as those of CO, CO_2 and hydrocarbon gases. In contrast, the yield of total water soluble product increased in the presence of NaOH because it reacted with CO_2 and formed soluble Na_2CO_3 and/or sodium acetate contained in the aqueous phase. It was observed that only NaOH affected the total gas yield significantly. For glucose, glutamic acid and mixture of these compounds, the hydrogen yield was significantly increased by the use of NaOH additive in subcritical water.

3.3. Characterization of catalyst residues from subcritical water gasification of glucose and glutamic acid in the presence of NaOH/Ni/Al₂O₃/Ni/SiO₂

The possibility of deactivation of the surface of Ni-based catalysts during the gasification of the model compounds under subcritical water conditions was examined using TGA, DTA, XRD and SEM techniques. The influence of NaOH as well as carbon deposits on the changes in the morphology and activities of Ni/Al_2O_3 and Ni/SiO_2 were investigated. The spent catalysts here refer to the solid residue collected from the filter paper after the filtration of the mixture of liquid and solid phase (reactor contents).

3.3.1. Spent catalyst characterization by X-ray diffraction (XRD)

The XRD spectra of the fresh are presented in Fig. 3. The freshly calcined Ni/Al_2O_3 and Ni/SiO_2 catalysts show the spectra corresponding to mainly Al_2O_3 and NiO in Fig. 3(a) and SiO_2 and NiO in Fig. 3(b), respectively. Analysis of the spent catalyst using XRD technique confirmed the presence of $NaAlCO_3(OH)_2$, dawsonite. The XRD scans in Fig. 4(a)–(c) show that spent catalysts from the reactions of glucose, glutamic acid and the mixture of glucose and glutamic acid with $NaOH/Ni/Al_2O_3$ contained AlO(OH), Ni and $NaAlCO_3(OH)_2$, respectively. No NiO was found which suggests that NiO was completely reduced to Ni as explained earlier. The combined NaOH and Ni/Al_2O_3 produced lower H_2 yield than NaOH alone even for glucose; possibly due to some of the NaOH reacting with Al_2O_3 to form dawsonite, as a result there was insufficient NaOH to promote the water–gas shift reaction to form H_2.

The XRD scans of spent catalysts Ni/SiO_2 and $NaOH–Ni/SiO_2$ combination detected mainly NiO and SiO_2 but no Ni (Fig. 5). The results did not show any compounds that could be formed from any reaction between NaOH and the catalyst. This may suggest that Ni/SiO_2 was more stable than Ni/Al_2O_3 under these experimental conditions. Furthermore, Table 5 shows that far less fixed carbon was found on the surface of Ni/SiO_2 than Ni/Al_2O_3 in the absence of NaOH. This also indicates that Ni/SiO_2 may be less prone to carbon poisoning than Ni/Al_2O_3. However, spent silica-supported catalyst contained more volatile matter than the alumina-supported catalyst.

Table 2
Mass balances for products obtained during subcritical water gasification of 5.0 g glucose at 330 °C, 120 min of reaction time and 1.5 wt% H_2O_2.

Sample type	Conc. NaOH (M)	H_2 (mg)	CO (mg)	CO_2 (mg)	C_1–C_4 gases (mg)	TWSP[a] (mg)	Tar (mg)	Solid residues[b] (mg)	H_2O (mg)	Mass balance (%)
Glucose 5.0 g	0.0	15.9	137	2100	25.9	331	550	680	2330	94.8
Glucose 5.0 g	1.0	138	5.91	222	12.2	6740	380	10.0	2390	94.3
Glucose 5.0 g + Ni/Al₂O₃	0.0	28.2	150	2790	38.8	68.2	470	1670	2610	104
Glucose 5.0 g + Ni/Al₂O₃	1.0	131	44.3	0.00	38.4	6540	80	1640	2000	91.1
Glucose 5.0 g + Ni/SiO₂	0.0	21.8	145	2290	41.3	187	430	1700	2540	98.0
Glucose 5.0 g + Ni/SiO₂	1.0	116	11.4	259	10.2	7080	280	1030	1990	93.6

[a] TWSP = total water soluble product.
[b] Solid residues including carbon, volatile matter and spent catalyst.

Table 3

Mass balances for products obtained during subcritical water gasification of 5.0 g glutamic Acid at 330 °C, 120 min of reaction time and 1.5 wt% H_2O_2.

Sample type	Conc. NaOH (M)	H_2 (mg)	CO (mg)	CO_2 (mg)	C_1–C_4 gases (mg)	NH_3 (mg)	N_2 (mg)	O_2 (mg)	TWSP [a] (mg)	Tar (mg)	Solid residues[b] (mg)	H_2O (mg)	Mass balance (%)
Glutamic acid	0.0	15.0	65.1	2600	0.00	282	1.00	0.0	792	520	0.0	2040	97.2
Glutamic acid	1.0	41.9	17.8	0.00	6.10	180	1.70	543	8520	150	160	1170	103
Glutamic acid + Ni/Al$_2$O$_3$	0.0	9.91	68.9	2680	371	306	0.91	57	936	480	1000	2150	103
Glutamic acid + Ni/Al$_2$O$_3$	1.0	34.3	14.6	1.80	3.01	182	1.50	353	7740	70.0	1660	1270	98.5
Glutamic acid + Ni/SiO$_2$	0.0	8.72	78.5	3020	43.8	321	0.82	0.0	1005	180	970	2440	108
Glutamic acid + Ni/SiO$_2$	1.0	30.1	15.6	152	3.11	224	1.43	353	8160	0.0	980	1120	96.0

[a] TWSP = total water soluble product.
[b] Solid residues including carbon, volatile matter and spent catalyst.

Table 4

Mass balances for products obtained during subcritical water gasification of 1:1 glucose/glutamic acid mixtures at 330 °C, 120 min of reaction time and 1.5 wt% H_2O_2.

Sample type	Conc. NaOH (M)	H_2 (mg)	CO (mg)	CO_2 (mg)	C_1–C_4 gases (mg)	NH_3 (mg)	N_2 (mg)	O_2 (mg)	TWSP [a] (mg)	Tar (mg)	Solid residues[b] (mg)	H_2O (mg)	Mass balance (%)
Glucose 2.5 g + glutamic acid 2.5 g	0.0	10.0	29.6	2793	18.9	114	0.60	40.3	211	1300	420	1810	104
Glucose 2.5 g + glutamic acid 2.5 g	1.0	121	11.0	0.00	4.1	163	0.40	0.00	7280	260	0.00	3280	106
Glucose 2.5 g + glutamic acid 2.5 g + Ni/Al$_2$O$_3$	0.0	14.5	109	3196	35.8	137	0.50	0.00	233	630	1400	1920	102
Glucose 2.5 g + glutamic acid 2.5 g + Ni/Al$_2$O$_3$	1.0	89.7	3.70	315	6.10	192	0.30	0.00	6910	0.00	1710	2430	101
Glucose 2.5 g + glutamic acid 2.5 g + Ni/SiO$_2$	0.0	16.3	95.8	3200	40.6	136	0.50	0.00	397	660	1290	1830	102
Glucose 2.5 g + glutamic acid 2.5 g + Ni/SiO$_2$	1.0	78.7	7.20	0.00	5.8	161	0.40	0.00	8580	90.0	1100	2140	106

[a] TWSP = total water soluble product.
[b] Solid residues including carbon, volatile matter and spent catalyst.
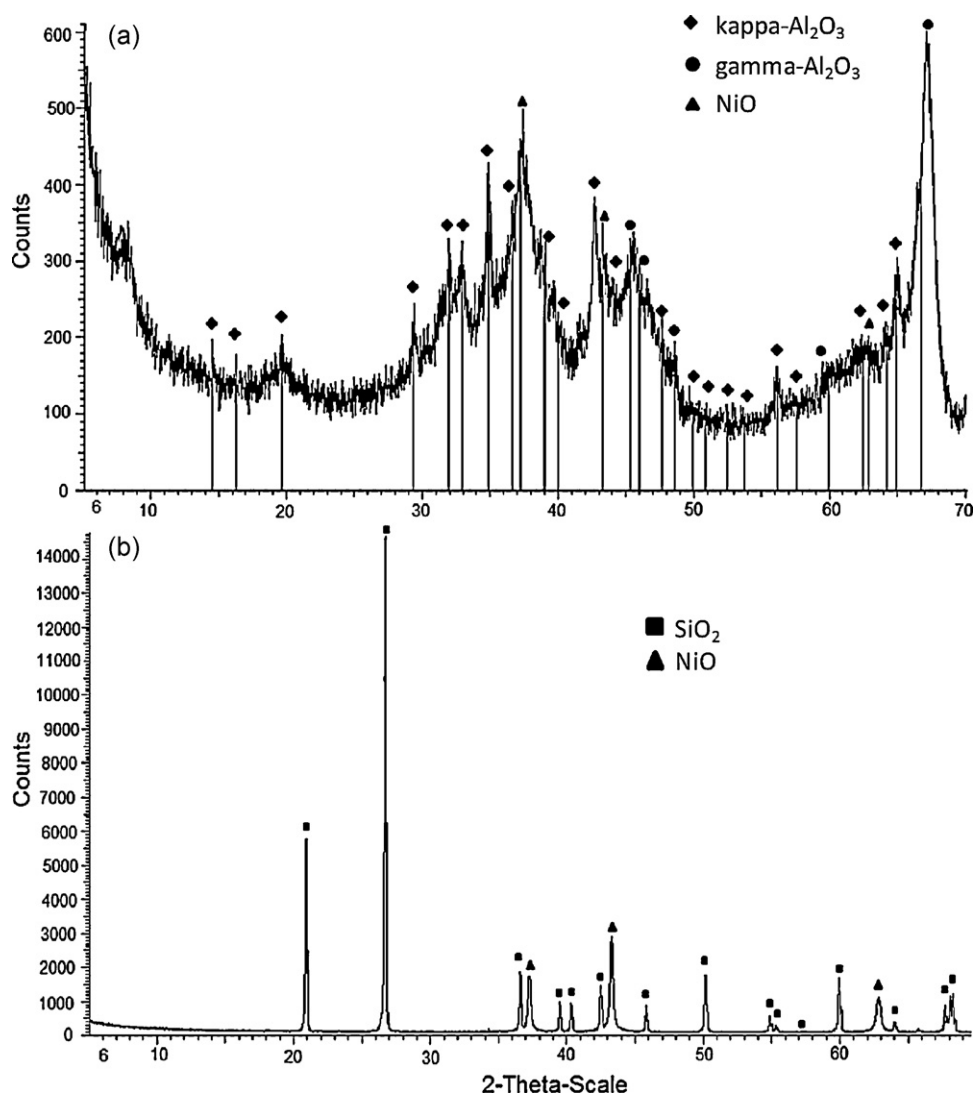
Fig. 3. XRD spectra of fresh catalysts (a) Ni/Al$_2$O$_3$ and (b) Ni/SiO$_2$.

Table 5
Proximate analysis of spent nickel catalysts and mixed catalysts (Ni/Al$_2$O$_3$ or Ni/SiO$_2$ with NaOH).

	% Weight loss				
	Moisture	Volatile compound	H$_2$O and CO$_2$ from dawsonite[a]	Fixed carbon	Ash/spent catalyst
Glucose (5 g = 100 wt%)					
Spent Ni/Al$_2$O$_3$	2.30	25.0	–	20.6	52.1
Spent Ni/SiO$_2$	1.15	43.1	–	4.23	51.8
Spent Ni/Al$_2$O$_3$ + NaOH	2.74	11.3	24.4	–	61.6
Spent Ni/SiO$_2$ + NaOH	4.29	14.1	–	–	81.7
Glutamic acid (5 g = 100 wt%)					
Spent Ni/Al$_2$O$_3$	1.44	10.1	–	–	88.5
Spent Ni/SiO$_2$	–	9.92	–	–	90.1
Spent Ni/Al$_2$O$_3$ + NaOH	6.97	10.3	19.9	–	62.8
SpentNi/SiO$_2$ + NaOH	6.57	9.33	–	–	84.2
Glucose/glutamic acid (2.5 g each = 50 wt% each)					
Spent Ni/Al$_2$O$_3$	1.13	23.5	–	4.84	70.5
Spent Ni/SiO$_2$	0.50	29.0	–	–	70.5
Spent Ni/Al$_2$O$_3$ + NaOH	3.00	–	38.0	–	59.0
Spent Ni/SiO$_2$ + NaOH	4.75	16.5	–	–	78.8

[a] Weight loss of H$_2$O and CO$_2$ from dawsonite (NaAlCO$_3$(OH)$_2$) decomposition in the temperature range 300 and 375 °C and between 360 and 675 °C.

3.3.2. Spent catalyst characterization by TGA and DTA

TGA analysis of the spent catalysts was carried out under nitrogen and air atmospheres to investigate the amount of moisture content, volatile and fixed carbon on the catalysts' surface and the results are presented in Table 5. The results show that the combination of NaOH, Ni/Al$_2$O$_3$ and Ni/SiO$_2$ yielded less volatile compound and carbon than either Ni/Al$_2$O$_3$ or Ni/SiO$_2$ catalyst alone. The data confirmed that the addition of NaOH alkali catalyst inhibited oil or char/coke formation in the gasification of the biomass model compounds [19,42,43].
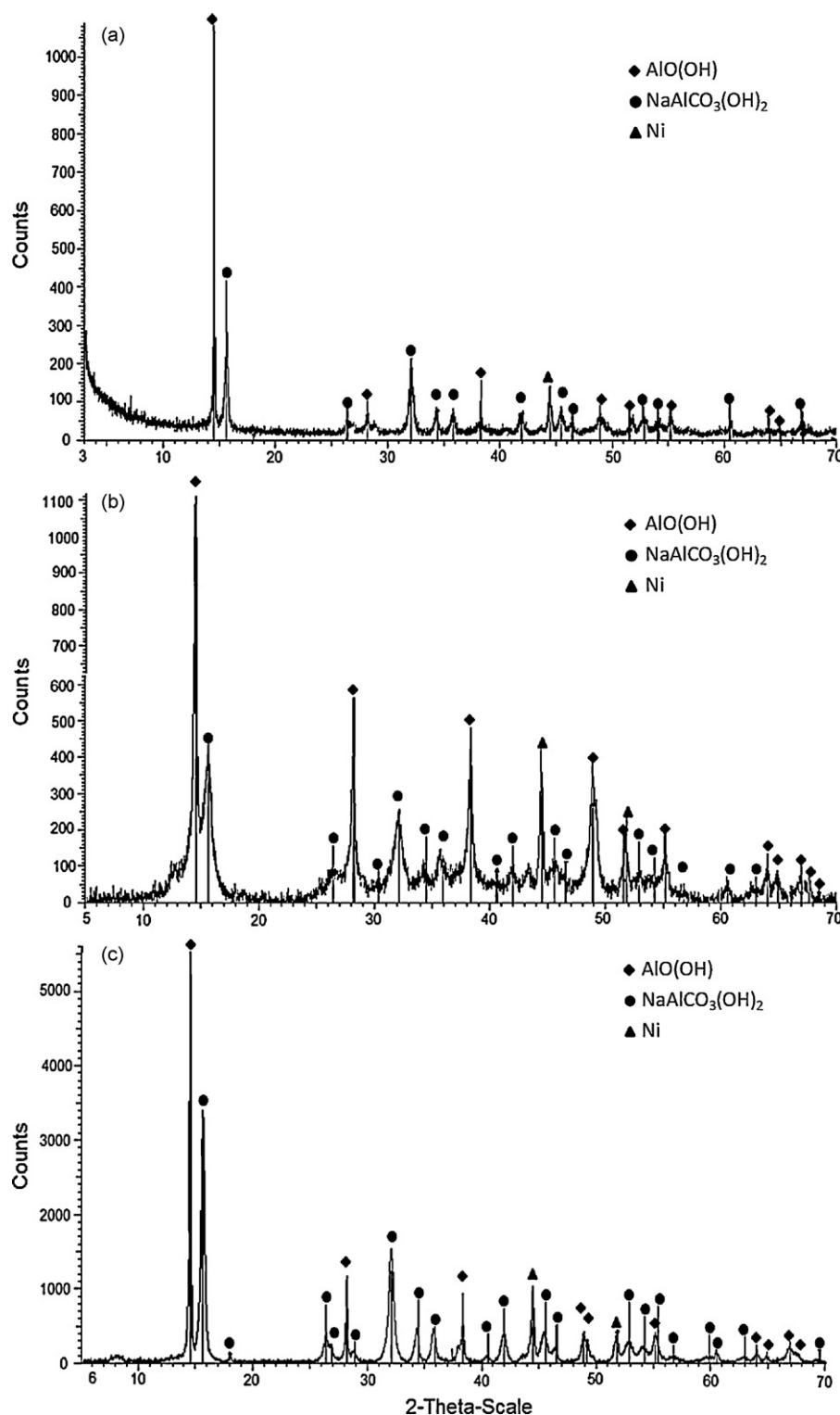
Fig. 4. XRD results of spent catalysts for subcritical water gasification in the presence NaOH and Ni/Al_2O_3 at 330 °C, 120 min and 1.5 wt% H_2O_2 (a) glucose only, (b) glutamic acid only, (c) 1:1 glucose/glutamic acid mixture.

From Table 5, subcritical water gasification using Ni/Al_2O_3 and Ni/SiO_2 without NaOH produced higher char and indeed, higher fixed carbon. The formation of volatile compounds/matter and carbon may have occurred from re-polymerization of degradation products of glucose and glutamic acid. The implication of carbon deposition on the catalyst surface of Ni/SiO_2 and Ni/Al_2O_3 is the loss of catalytic activity through deactivation of these catalysts [27]. This could essentially lead to a decrease in hydrogen production.

However, huge differences existed between the products obtained from the gasification of glucose and glutamic acid, respectively in the presence of NaOH, Ni/Al_2O_3, Ni/SiO_2 and mixtures of the Ni-based catalysts and NaOH. It thus became important to investigate the causes of these observations.

During DTA studies, solid residues produced during the reactions of glucose and glutamic acid, in the presence of NaOH and Ni/Al_2O_3 showed very significant losses in the region expected
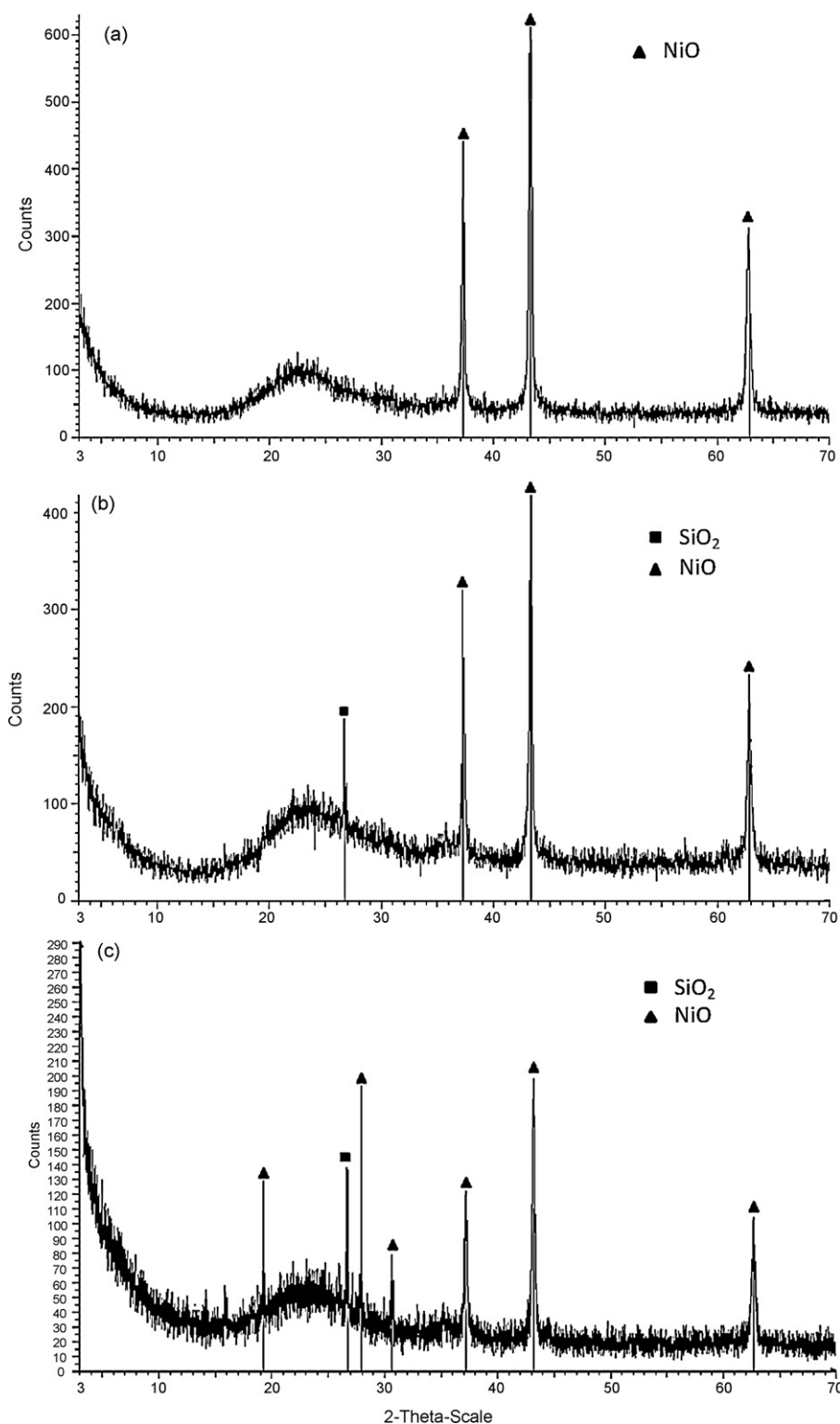
Fig. 5. XRD results of spent catalysts for subcritical water gasification in the presence of NaOH with Ni/SiO$_2$ at 330 °C, 120 min and 1.5 wt% H$_2$O$_2$ (a) glucose only, (b) glutamic acid only, (c) 1:1 glucose/glutamic acid mixture.

for volatile compounds compared to residues obtained without NaOH. DTA analysis, carried out in the decomposition range of temperature 120–850 °C clearly showed differences between spent Ni/Al$_2$O$_3$ catalysts used with and without NaOH. From the DTA analysis shown in Fig. 6, in all cases of samples gasified with and without NaOH catalyst, there is one predominantly different decomposition peak of spent Ni/Al$_2$O$_3$ catalysts occurring between

150 and 400 °C. The spent Ni/Al$_2$O$_3$ catalyst without NaOH has only volatile compounds in this temperature range. The decomposition of dawsonite has been studied by Huggins and Green [44] and Stoica et al. [45], who reported the decomposition products to include H$_2$O, CO$_2$, and NaAlO$_2$ as illustrated in Eq. (11). Huggins and Green [44] showed that the decomposition involved a two-step reaction. In the first step, the crystalline dawsonite decomposes

Table 6
BET surface area of the Ni/Al$_2$O$_3$ catalysts before and after use in the gasification experiments, with and without NaOH additive.

Catalysts + conditions	BET surface area (m^2/g)
Fresh Ni/Al$_2$O$_3$	94.8
Spent catalysts	
Ni/Al$_2$O$_3$ without sample	71.4
Ni/Al$_2$O$_3$ + NaOH without sample	58.3
Ni/Al$_2$O$_3$ + glucose	27.6
Ni/Al$_2$O$_3$ + NaOH + glucose	7.99
Ni/Al$_2$O$_3$ + glutamic acid	49.5
Ni/Al$_2$O$_3$ + NaOH + glutamic acid	27.8

between 300 and 375 °C. In this step the dawsonite loses all the adsorbed water molecules and a large portion of CO$_2$. In the second, which is a slower step, the remaining CO$_2$ is released over the range of 360–650 °C producing crystalline sodium aluminate (NaAlO$_2$) formed at approximately 670 °C [44].

Dawsonite decomposition:

$$NaAlCO_3(OH)_2 \rightarrow H_2O + CO_2 + NaAlO_2 \tag{11}$$

From the DTA results shown in Fig. 6, thus the spent Ni/Al$_2$O$_3$ catalysts with NaOH might consist of not only volatile compounds but also dawsonite decomposition considered from 120 to 850 °C. As a result the decomposition peak of dawsonite and volatile compounds would likely overlap. Therefore the weight loss of apparent volatile compounds and H$_2$O and CO$_2$ from dawsonite decomposition was separately determined. Between temperature of 300 and 375 °C and between 360 and 675 °C, the weight loss of H$_2$O and CO$_2$ evolved was calculated and then deducted from total weight loss in this temperature range to obtain the weight loss of apparent volatile compounds (Table 5). Hence, it was found that much of the weight losses was attributable to the decomposition of dawsonite rather that actual losses of volatile organic compounds.

3.3.3. BET analysis of spent catalyst

The surface area of the spent catalyst was analysed by BET method as illustrated in Table 6, which shows that the surface area of Ni/Al$_2$O$_3$ significantly decreased in the presence of NaOH. However, it was important to identify the major cause of this observation. A set of experiments was carried out under identical conditions except that Ni/Al$_2$O$_3$, with and without NaOH, was loaded into the reactor in the absence of either glucose or glutamic acid. BET analysis of the solid residue obtained showed that the surface area of the spent Ni/Al$_2$O$_3$ decreased by about 38.5% when reacted with NaOH. In the absence of NaOH, the surface area decreased by 24.7%, possibly due to the reaction of Al$_2$O$_3$ with hot water to produce Al(OH)$_3$. In the presence of glucose or glutamic acid, the surface area of Ni/Al$_2$O$_3$ catalysts decreased dramatically possibly as a result of dawsonite formation and deactivation by carbon deposits. In case of 5 g glucose, the surface area reduced by 91.6 and 70.9%, respectively with and without NaOH. For 5 g glutamic acid, the surface area decreased by 70.7 and 47.8%, respectively. Hence, it is obvious that in all cases, larger decrease of Ni/Al$_2$O$_3$ surface area was observed in the presence of NaOH compared to when NaOH was absent, indicating the possibility of reactions between the two catalysts. The formation of dawsonite could have resulted from the following reaction schemes:
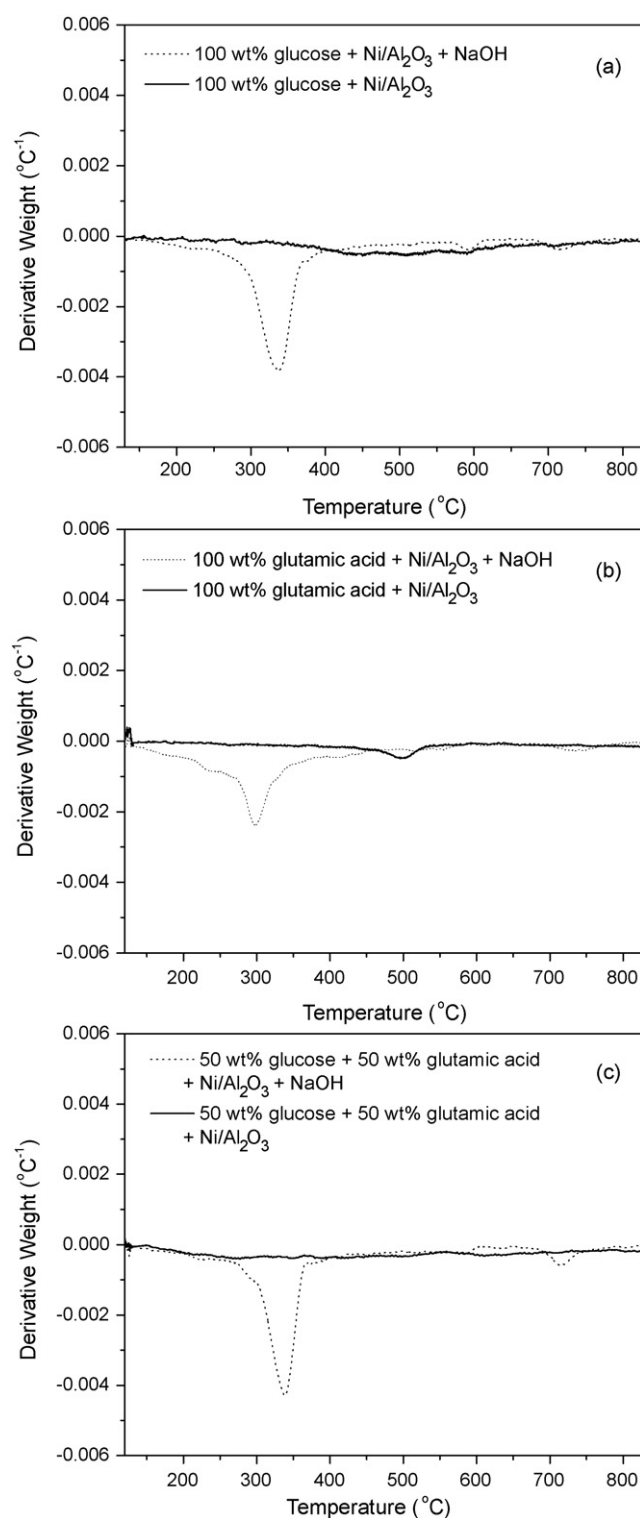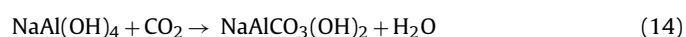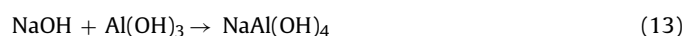
$$3H_2O + Al_2O_3 \rightarrow 2Al(OH)_3 \tag{12}$$

$$NaOH + Al(OH)_3 \rightarrow NaAl(OH)_4 \tag{13}$$

$$NaAl(OH)_4 + CO_2 \rightarrow NaAlCO_3(OH)_2 + H_2O \tag{14}$$

Fig. 6. DTA analysis of spent Ni/Al$_2$O$_3$ catalysts with and without NaOH collected after subcritical water gasification at 330 °C, 120 min and 1.5 wt% H$_2$O$_2$ (a) glucose only, (b) glutamic acid only, (c) 1:1 glucose/glutamic acid mixture.

The reaction of alumina with hot water would lead to the production of aluminium hydroxide as shown in Eq. (12). Variations of this compound in the form of AlO(OH) as shown in the XRD scans can also be possible. The reaction of sodium hydroxide with alumina or aluminium hydroxide (Eq. (13)) to form soluble sodium aluminate is very well known reaction for which many drain cleaners are based. However, this amphoteric NaAl(OH)$_4$ could react
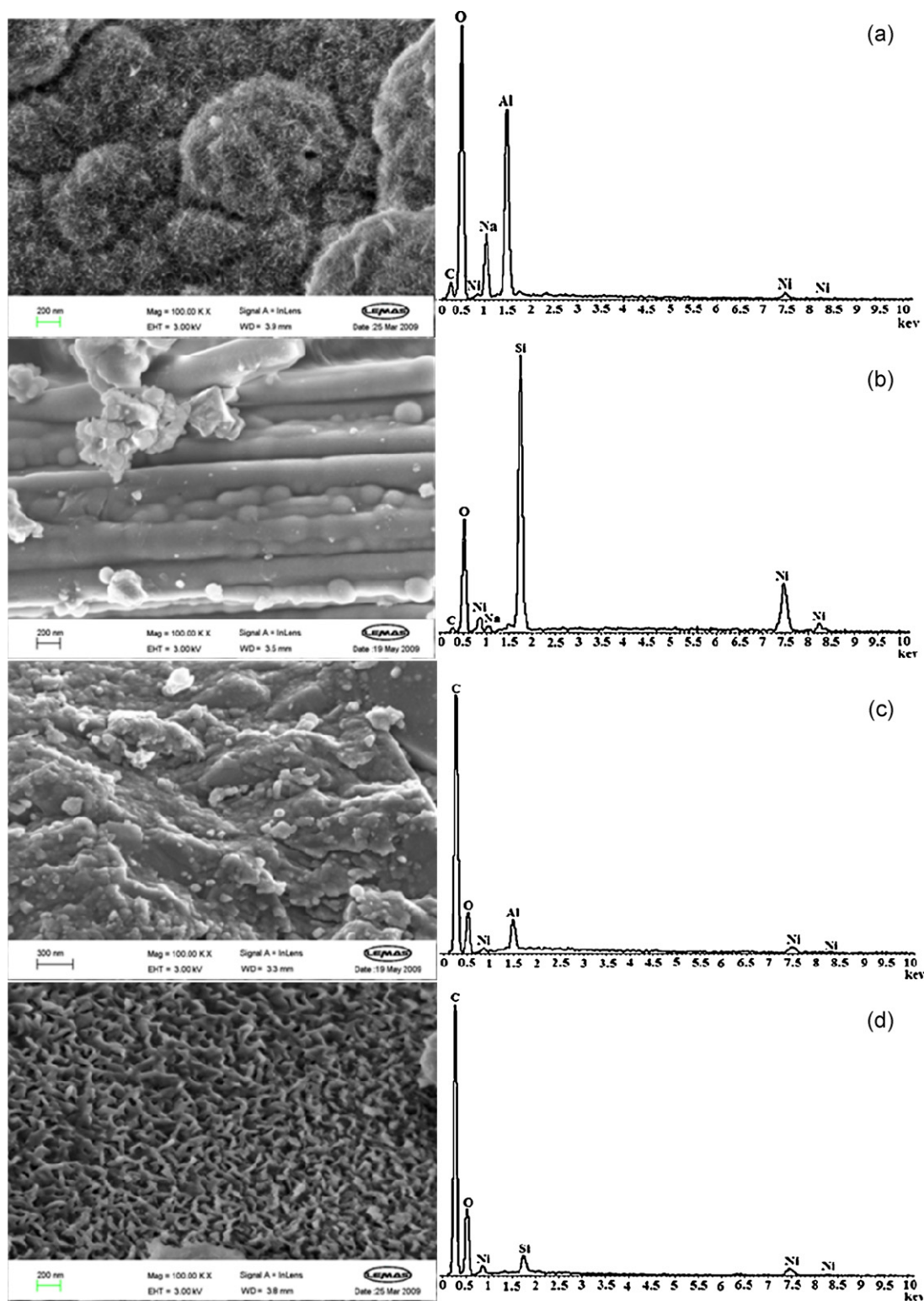
Fig. 7. SEM and EDXS analysis of solid residues from subcritical water gasification of glucose at 330 °C and 120 min (sample size, 5 g/1.5 wt% H_2O_2 each) (a) Ni/Al_2O_3 with NaOH, (b) Ni/SiO_2 with NaOH, (c) only Ni/Al_2O_3, (d) only Ni/SiO_2.

with acidic carbon dioxide or carbonates to produce dawsonite as shown in Eq. (14). The geochemical and laboratory production of dawsonite under hydrothermal conditions have been widely reported in literature [46–49]. Moreover, the formation of dawsonite could result from the reaction of aluminium hydroxide and

sodium bicarbonate directly as shown below [48]:

$$Al(OH)_3 + NaHCO_3 \rightarrow NaAlCO_3(OH)_2 + H_2O \qquad (15)$$
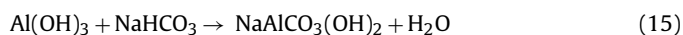
Most importantly, in this paper the formation of dawsonite, $NaAlCO_3(OH)_2$, is an indication of the occurrence of side reactions
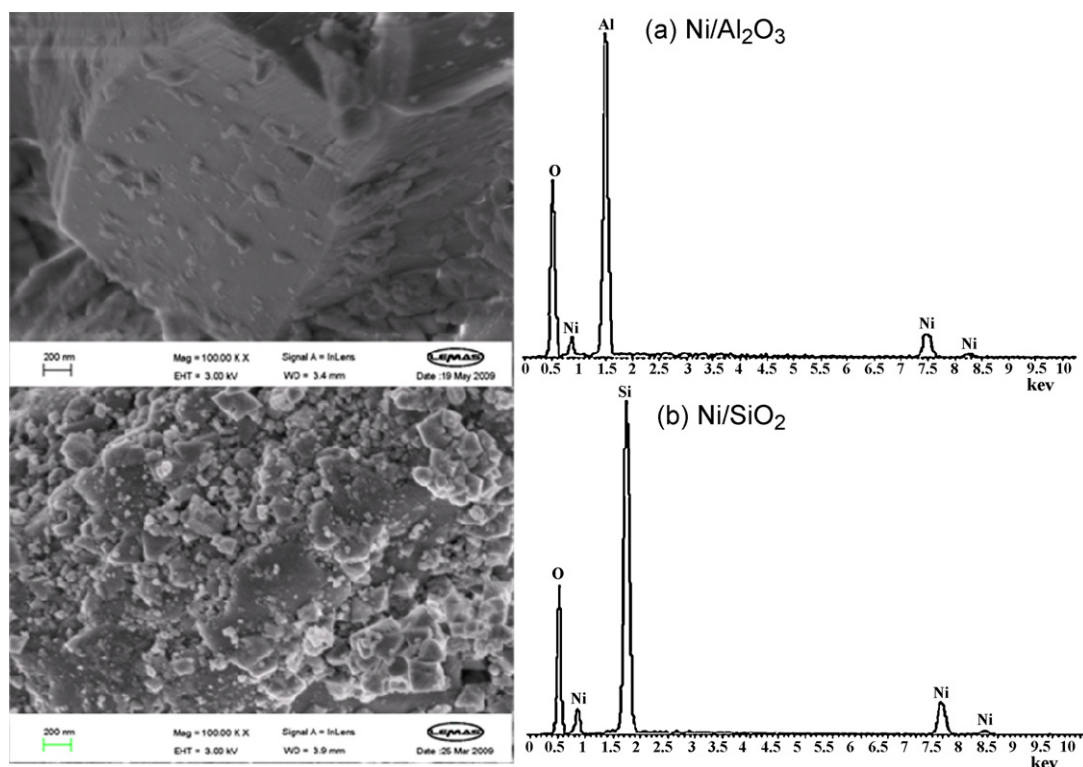
Fig. 8. SEM images and EDXS results of the fresh catalysts.

which could potentially reduce the activity of both the Ni/Al_2O_3 catalyst and NaOH additive.

3.3.4. Spent catalyst characterization by SEM/EDXS

The EDXS results presented in Fig. 7 shows a small peak of carbon, C detected in the catalyst residue involving the use of NaOH and Ni/Al_2O_3. This C peak might be volatile compound and/or C contained in dawsonite. Meanwhile, the significantly high peak of C in the absence of NaOH contains both volatile compounds and fixed carbon. If the percentage of fixed carbon was ignored, the C peak of the spent Ni/Al_2O_3 catalyst without NaOH would still be higher. This could suggest that little or no volatile compounds were associated to the spent catalyst involving the addition of NaOH. Hence the decomposition dawsonite must have contributed immensely to apparent volatile matter losses when Ni/Al_2O_3 was used with NaOH.

The changes in the characteristics of the nickel catalysts can clearly be seen by comparing the SEM images and EDXS results of the spent catalysts in Fig. 7 to similar images of the fresh catalysts in Fig. 8. The EDXS results in Fig. 7 shows the main elements of each solid residue containing Ni, Na, Al, Si, O and C. The carbon peak responses from the EDXS results could be used to support the formation of hydrocarbons (volatile compounds) and fixed carbon on the solid residue surface corresponding with results shown in Table 5. The solid residue produced by using Ni/Al_2O_3 or Ni/SiO_2 alone has the highest carbon peak. SEM images also clearly show domains of carbon on the Ni/Al_2O_3 catalyst surface (Fig. 7(c)) and deposited filamentous carbon observed on Ni/SiO_2 (Fig. 7(d)). Although SEM images could not clearly indicate carbon deposition in the case of the combination of NaOH with Ni/Al_2O_3 or Ni/SiO_2 shown in Fig. 7(a) and (b), respectively, EDXS results showed that the high carbon signal was significantly decreased when the additive NaOH was utilized.

4. Conclusions

The production of hydrogen via subcritical water gasification of glucose and glutamic acid as model compounds has been investigated. The influence of NaOH additive, Ni/Al_2O_3 and Ni/SiO_2 catalysts and the combination of these catalysts in relation to hydrogen production was examined. Increasing concentration of NaOH enhanced the important decomposition reactions of the model compounds and also promoted the water gas shift reaction leading to higher H_2, lower CO_2 production and a CO-lean gas product. Also, the amount of oil/tar and char decreased in the presence of NaOH additive. The NaOH could promote glucose decomposition to water soluble products and CO formation. The product CO_2 reacted with NaOH so that the concentration of CO_2 decreased and was responsible for shifting the water–gas reaction in the forward direction. Glutamic acid appeared to be decomposed mainly via decarboxylation to produce CO_2, which reacted to consume the added alkali. The consumption of the alkali by these side reactions rendered it unavailable for the type of hydrothermal decomposition reaction that would produce gasifiable intermediates.

Using the NaOH catalyst in the subcritical water gasification in the presence of Ni/Al_2O_3 and Ni/SiO_2 led to a higher production of H_2 gas and reduction of CO_2 gas, compared to the nickel catalysts alone, respectively. Added NaOH also decreased the amount of hydrocarbon compounds and carbon deposited on the solid catalyst surface. With NaOH, CO was reduced because it was consumed via the water–gas shift reaction. Therefore, NaOH was much more effective than either of Ni/Al_2O_3 and Ni/SiO_2 to generate H_2 gas under the test conditions. There was reasonable evidence to mention that sintering of the Ni/Al_2O_3 occurred in the presence of NaOH due to chemical reaction between them to produce dawsonite found on the spent catalyst.

Acknowledgements

References

[1] M. Watanabe, H. Inomata, K. Arai, Biomass Bioenergy 22 (2002) 405.
[2] J. Yanik, S. Ebale, A. Kruse, M. Saglam, M. Yuksel, Fuel 86 (2007) 2410.
[3] A. Kruse, J. Supercrit. Fluids 47 (2009) 391.
[4] A. Kruse, Biofuel Bioprod. Biorefin. 2 (2008) 415.
[5] G.J. DiLeo, M.E. Neff, S. Kim, P.E. Savage, Energy Fuels 22 (2008) 871.
[6] A. Loppinet-Serani, C. Aymonier, F. Cansell, ChemSusChem 1 (2008) 486.
[7] J. Douda, V.A. Basiuk, J. Anal. Appl. Pyrol. 56 (2000) 113.
[8] D. Xu, S. Wang, X. Hu, C. Chen, Q. Zhang, Y. Gong, Int. J. Hydrogen Energy 34 (2009) 5357.
[9] Y. Ishida, K. Kumabe, K. Hata, K. Tanifuji, T. Hasegawa, K. Kitagawa, N. Isu, Y. Funahashi, T. Asai, Biomass Bioenergy 33 (2009) 8.
[10] D.J. Adams, P.J. Dyson, S.J. Tavener, Chemistry in Alternative Reaction Media, John Wiley & Sons Ltd., UK, 2004.
[11] P. Krammer, H.J. Vogel, Supercrit. Fluids 16 (2000) 189.
[12] A. Kruse, A. Gawlik, Ind. Eng. Chem. Res. 42 (2003) 267.
[13] J.M. Kremser, C.O. Kappe, Eur. J. Org. Chem. 324 (2005) 3672.
[14] Y. Calzavara, C. Joussot-Dubien, G. Boissonnet, S. Sarrade, Energy Convers. Manage. 46 (2005) 615.
[15] M. Goto, R. Obuchi, T. Hirose, T. Sakaki, M. Shibata, Bioresour. Technol. 93 (2004) 279.
[16] P.T. Williams, J.A. Onwudili, Energy Fuels 20 (2006) 1259.
[17] P.E. Savage, Chem. Rev. 99 (1999) 603.
[18] K. Kruse, A. Krupka, V. Schwarzkopf, C. Gamard, T. Henningsen, Ind. Eng. Chem. Res. 44 (2005) 3013.
[19] J.A. Onwudili, P.T. Williams, Int. J. Hydrogen Energy 34 (2009) 5645.
[20] G.V. Rossum, B. Potic, S.R.A. Kersten, W.P.M.V. Swaaij, Catal. Today 145 (2009) 10.
[21] J. Yanik, S. Ebale, A. Kruse, M. Saglam, M. Yüksel, Int. J. Hydrogen Energy 33 (2008) 4520.
[22] J.R. Rostrup-Nielsen, J.H. Hensen, J. Catal. 144 (1993) 38.
[23] F. Pompeo, N.N. Nichio, M.M.V.M. Souza, D.V. Cesar, O.A. Ferretti, M. Schmal, Appl. Catal. A: Gen. 316 (2007) 175.
[24] D. Sutton, B. Kelleher, J.R.H. Ross, Fuel Proc. Technol. 73 (2001) 155.
[25] Z.A. El-Rub, E.A. Bramer, G. Brem, Ind. Eng. Chem. Res. 43 (2004) 6911.
[26] P. Simell, J. Hepola, A. Krause, Fuel 76 (1997) 1117.
[27] J. Srinakruang, K. Sato, T. Vitidsant, K. Fujimoto, Catal. Commun. 6 (2005) 437.
[28] A. Sinag, A. Kruse, J. Rathert, Ind. Eng. Chem. Res. 43 (2004) 502.
[29] I. Lee, M. Kim, S. Ihm, Ind. Eng. Chem. Res. 41 (2002) 1182.
[30] J. Xu, G.F. Froment, AIChE J. 35 (1989) 88.
[31] H. Habazaki, M. Yamasaki, B.P. Zhang, A. Kawashima, S. Kohno, T. Takai, K. Hashimoto, Appl. Catal. A: Gen. 172 (1998) 131.
[32] M. Agnelli, H.M. Swaan, C. Marquez-Alvarez, G.A. Martin, C. Mirodatos, J. Catal. 175 (1998) 117.
[33] M.T. Tavares, I. Alstrup, C.A. Bernardo, J.R. Rostrup-Nielsen, J. Catal. 158 (1996) 402.
[34] Y.C. Fu, K. Ishikuro, T. Fueta, M. Akiyoshi, Energy Fuels 9 (1995) 406.
[35] T. Yoshida, Y. Oshima, Y. Matsumura, Biomass Bioenergy 26 (2004) 71.
[36] T. Yoshida, Y. Matsumura, Ind. Eng. Chem. Res. 40 (2001) 5469.
[37] T. Minowa, T. Ogi, S. Yokoyama, Chem. Lett. 24 (1995) 937.
[38] T. Minowa, T. Ogi, Catal. Today 45 (1998).
[39] H. Schmieder, J. Abeln, N. Boukis, E. Dinjus, A. Kruse, M. Kluth, G. Petrich, E. Sadri, M. Schacht, J. Supercrit. Fluids 17 (2000) 145.
[40] N. Sato, A.T. Quitain, K. Kang, H. Daimon, K. Fujie, Ind. Eng. Chem. Res. 43 (2004) 3217.
[41] Z. Fang, T. Minowa, C. Fang, R.L. Smith, H. Inomato, J.A. Kozinnski, Int. J. Hydrogen Energy 33 (2008) 981.
[42] A. Sinag, A. Kruse, A. Schwarzkopf, Eng. Life Sci. 3 (2003) 469.
[43] A. Kruse, T. Henningsen, A. Sinag, J. Pfeiffer, Ind. Eng. Chem. Res. 42 (2003) 3711.
[44] C.W. Huggins, T.E. Green, Am. Miner. 58 (1973) 548.
[45] G. Stoica, S. Abello, J. Perez-Ramirez, Appl. Catal. A: Gen. 365 (2009) 252.
[46] R.M. Coveney, W.C. Kelly, Miner. Petrol. 32 (1971) 334.
[47] E. Alvarez-Ayuso, H.W. Nugteren, Water Res. 39 (2005) 2096.
[48] J. Moore, J. Adams, R. Allis, S. Lutz, S. Rauzi, Chem. Geol. 217 (2005) 365–385.
[49] S. Walspurger, P.D. Cobben, W.G. Haije, R. Westerwaal, G.D. Elzinga, O.V. Safonova, Eur. J. Inorg. Chem. 263 (2010) 2461.